Exact solutions for unsteady axial Couette flow of a fractional Maxwell fluid due to an accelerated shear

Muhammad Athar [a], **Corina Fetecau** [b], **Muhammad Kamran** [c], **Ahmad Sohail** [a], **Muhammad Imran** [a]

[a] Abdus Salam School of Mathematical Sciences, GC University
Lahore, Pakistan
drmimranchaudhry@gmail.com

[b] Department of Theoretical Mechanics, Technical University of Iasi
Iasi, Romania

[c] COMSATS Institute of Information Technology
Wah Cantt, Pakistan

Received: 19 February 2011 / **Revised:** 20 April 2011 / **Published online:** 30 May 2011

Abstract. The velocity field and the adequate shear stress corresponding to the flow of a fractional Maxwell fluid (FMF) between two infinite coaxial cylinders, are determined by means of the Laplace and finite Hankel transforms. The motion is produced by the inner cylinder that at time $t = 0^+$ applies a shear stress ft^a $(a \geq 0)$ to the fluid. The solutions that have been obtained, presented under series form in terms of the generalized G and R functions, satisfy all imposed initial and boundary conditions. Similar solutions for ordinary Maxwell and Newtonian fluids are obtained as special cases of general solutions. The unsteady solutions corresponding to $a = 1, 2, 3, \ldots$ can be written as simple or multiple integrals of similar solutions for $a = 0$ and we extend this for any positive real number a expressing in fractional integration. Furthermore, for $a = 0, 1$ and 2, the solutions corresponding to Maxwell fluid compared graphically with the solutions obtained in [1–3], earlier by a different technique. For $a = 0$ and 1 the unsteady motion of a Maxwell fluid, as well as that of a Newtonian fluid ultimately becomes steady and the required time to reach the steady-state is graphically established. Finally a comparison between the motions of FMF and Maxwell fluid is underlined by graphical illustrations

Keywords: fractional Maxwell fluid, exact solutions, velocity field, shear stress.

1 Introduction

The motion of a fluid in cylindrical domains has applications in the food industry, oil exploitation, chemistry and bio-engineering [4]. The non-Newtonian fluids are now considered to play a more important and appropriate role in technological applications in comparison with Newtonian fluids. The first exact solutions corresponding to motions of non-Newtonian fluids in cylindrical domains seem to be those of Ting [5] for second grade fluids, Srivastava [6] for Maxwell fluids and Waters and King [7] for Oldroyd-B fluids. To the best of our knowledge, the first exact solutions for motions of non-Newtonian fluids due to a shear stress on the boundary are those of Bandelli and Rajagopal [8] and Bandelli et al. [9] for second grade fluids and Waters and King [10] for Oldroyd-B fluids. Other similar solutions have been recently obtained in [11, 12]. The solutions from [8], obtained by means of the Laplace transform, give the velocity field corresponding to the motion of second grade fluid between two infinite circular cylinders.

In this paper, our interest is to find the velocity field and the shear stress corresponding to the motion of a Maxwell fluid between two infinite circular cylinders, one of them being subject to a longitudinal time-dependent shear stress ft^a, $a \geq 0$. In the last time, the fractional calculus has encountered much success in description of complex dynamics such as relaxation, oscillation, wave and viscoelastic behavior. Several authors suggested that the integral-order models for viscoelastic materials seem to be inadequate, especially from the qualitative point of view. In the same time they proposed fractional-order laws of deformation for modeling the viscoelastic behavior of real materials. One of them

$$\sigma(t) = \mu_s D_t^1\big[\varepsilon(t)\big] + \left[\frac{3}{2}(\mu_0 - \mu_s)nKT\right]^{\frac{1}{2}} D_t^{\frac{1}{2}}\big[\varepsilon(t)\big],$$

due to Rouse [13], is used in the molecular theory for dilute polymer solutions. Here σ is the stress, ε the strain, μ_s is the steady-flow viscosity of the solvent, μ_0 is the steady-flow viscosity of the solution, n is the number of molecules, K is the Boltzman constant, T is the absolute temperature and D_t^α is a fractional differential operator to be defined in the next section. Ferry et al. [14], modified the Rouse theory in concentrated polymer solutions and polymer solids with no cross-linking and obtained that

$$\sigma(t) = \left[\frac{3\mu\rho RT}{2M}\right]^{\frac{1}{2}} D_t^{\frac{1}{2}}\big[\varepsilon(t)\big],$$

where μ is the viscosity, ρ the density, R is the universal gas constant and M the molecular weight. Consequently, the fractional calculus approach to viscoelasticity for the study of viscoelastic material properties is justified, at least for polymer solutions and for polymer solids without cross-linking. In the meantime, a lot of exact solutions corresponding to different motions of non-Newtonian fluids with fractional derivatives have been established, but we mention here only a few in cylindrical domains [15–18]. Furthermore, the one-dimensional fractional derivative Maxwell model has been found very useful in modeling the linear viscoelastic response of some polymers in the glass transition and the glass state [19]. It is worth pointing out that Palade et al. [20] developed a fully objective constitutive equation for an incompressible fluid-reducible to the linear fractional derivative Maxwell model under small deformations hypothesis. For a deeper documentation on this subject, one can also see the books [21, 22].

Consequently, for completeness and motivated by the above remarks, we solve our problem for fractional Maxwell fluids (FMF). The solutions that have been obtained, presented under series form in terms of $G_{a,b,c}(\cdot, t)$ and $R_{a,b}(\cdot, t)$ generalized functions, satisfy both governing equations and all imposed initial and boundary conditions. They can be easy specialized to give the similar solutions for ordinary Maxwell and Newtonian fluids. Some important properties are obtained for the special cases $a = 0, 1, 2$, and the required time to reach the steady-state or the large-time state is graphically established.

2 Basic governing equations

The flows to be here studied have the velocity field $\mathbf{v}$ and the extra-stress $\mathbf{S}$ of the form

$$\mathbf{v} = \mathbf{v}(r,t) = v(r,t)\mathbf{e}_z, \tag{1a}$$
$$\mathbf{S} = \mathbf{S}(r,t), \tag{1b}$$

where $\mathbf{e}_z$ is the unit vector in the z-direction of the cylindrical coordinate system r, θ and z. For such flows the constraint of incompressibility is automatically satisfied while the governing equations corresponding to fractional Maxwell fluid (FMF) are [18]

$$\left(1+\lambda D_t^\alpha\right)\frac{\partial v(r,t)}{\partial t} = \nu\left(\frac{\partial^2}{\partial r^2}+\frac{1}{r}\frac{\partial}{\partial r}\right)v(r,t), \tag{2a}$$
$$\left(1+\lambda D_t^\alpha\right)\tau(r,t) = \mu\frac{\partial v(r,t)}{\partial r}, \tag{2b}$$

where $\tau(r,t) = S_{rz}(r,t)$ is the non-trivial shear stress, λ is a material constant, μ is the dynamic viscosity, $\nu = \mu/\rho$ is the kinematic viscosity (ρ being the constant density of the fluid) and the fractional differential operator D_t^α is defined by [23, 24]

$$D_t^\alpha f(t) = \frac{1}{\gamma(1-\alpha)}\frac{\mathrm{d}}{\mathrm{d}t}\int_0^t \frac{f(\tau)}{(t-\tau)^\alpha}\,\mathrm{d}\tau, \quad 0 \le \alpha < 1, \tag{3}$$

and $\Gamma(.)$ is the gamma function. Of course the material constant λ has the dimension of t^α and for $\alpha \to 1$ it tends to the relaxation time. In the following the fractional partial differential equations (2), with appropriate initial and boundary conditions, will be solved by means of Hankel and Laplace transforms. In order to avoid lengthy calculations of residues and contours integrals, the discrete inverse Laplace transform method will be used [15–18].

3 Axial Couette flow between two infinite cylinders

Let us consider an incompressible FMF at rest in an annular region between two coaxial circular cylinders of radii R_1 and R_2 ($R_2 > R_1$). At time $t = 0^+$, a time-dependent longitudinal shear stress

$$\tau(R_1,t) = \frac{f\Gamma(a+1)}{\lambda}R_{\alpha,-a-1}\left(\frac{-1}{\lambda},t\right), \quad 0 < \alpha < 1, \;\; a \ge 0, \tag{4}$$

where f is a real constant and the generalized $R_{a,b}(c,t)$ functions are defined by [25]

$$R_{a,b}(c,t) = \mathcal{L}^{-1}\left\{\frac{q^b}{q^a - c}\right\} = \sum_{n=0}^{\infty} \frac{c^n t^{(n+1)a-b-1}}{\Gamma[(n+1)a-b]}, \tag{5}$$
$$\operatorname{Re}(a-b) > 0, \ \ \operatorname{Re}(q) > 0,$$

is applied on the boundary of the inner cylinder. Due to the shear, the fluid is gradually moved. Its velocity is of the form (1a) and the governing equations are given by Eqs. (2). The appropriate initial and boundary conditions are

$$v(r,0) = \frac{\partial v(r,0)}{\partial t} = 0, \quad r \in (R_1, R_2], \tag{6a}$$

$$\tau(r,0) = 0, \quad r \in (R_1, R_2], \tag{6b}$$

and

$$\left(1 + \lambda D_t^\alpha\right)\tau(r,t)\big|_{r=R_1} = \mu \frac{\partial v(r,t)}{\partial r}\bigg|_{r=R_1} = f t^a, \quad t \geq 0, \tag{7a}$$

$$v(R_2, t) = 0, \quad t \geq 0. \tag{7b}$$

Of course, as we shall later see, $\tau(R_1,t)$ given by Eq. (4) is just the solution of the fractional differential equation (7a). For $\alpha \to 1$, Eq. (4) takes the simple form

$$\tau(R_1,t) = \frac{f}{\lambda}\int_0^t (t-s)^a \exp\left(\frac{-s}{\lambda}\right) \mathrm{d}s = \frac{f}{\lambda}\Gamma(a+1) R_{1,-a-1}\left(\frac{-1}{\lambda}, t\right), \tag{8}$$

corresponding to ordinary Maxwell fluids.

3.1 Calculation of the velocity field

Applying the Laplace transform to Eq. (2b), using the Laplace transform formula for sequential fractional derivatives [24] and having the initial and boundary conditions (6) and (7) in mind, we find that

$$\left(q + \lambda q^{\alpha+1}\right)\overline{v}(r,q) = \nu\left(\frac{\partial^2}{\partial r^2} + \frac{1}{r}\frac{\partial}{\partial r}\right)\overline{v}(r,q), \quad r \in (R_1, R_2), \tag{9}$$

where the image function $\overline{v}(r,q) = \mathcal{L}\{v(r,t)\}$ has to satisfy the conditions

$$\frac{\partial \overline{v}(r,q)}{\partial r}\bigg|_{r=R_1} = \frac{f\Gamma(a+1)}{\mu q^{a+1}} \quad \text{and} \quad \overline{v}(R_2, q) = 0. \tag{10}$$

In the following we shall denote by [26]

$$\overline{v}_H(r_n, q) = \int_{R_1}^{R_2} r\overline{v}(r,q) B(r, r_n)\, \mathrm{d}r, \tag{11}$$

the Hankel transform of $\overline{v}(r,q)$, where

$$B(r,r_n) = J_0(rr_n)Y_1(R_1r_n) - J_1(R_1r_n)Y_0(rr_n), \tag{12}$$

r_n are the positive roots of the transcendental equation $B(R_2,r) = 0$, while $J_p(.)$ and $Y_p(.)$ are Bessel functions of the first and second kind of order p. The inverse Hankel transform of $\overline{v}_H(r_n,q)$ is given by [26]

$$\overline{v}(r,q) = \frac{\pi^2}{2}\sum_{n=1}^{\infty}\frac{r_n^2 J_0^2(R_2r_n)B(r,r_n)}{J_1^2(R_1r_n) - J_0^2(R_2r_n)}\,\overline{v}_H(r_n,q). \tag{13}$$

Multiplying both sides of Eq. (9) by $rB(r,r_n)$, integrating with respect to r from R_1 to R_2 and taking into account the conditions (6), and using the result

$$\int_{R_1}^{R_2} r\left[\frac{\partial^2\overline{v}(r,q)}{\partial r^2} + \frac{1}{r}\frac{\partial\overline{v}(r,q)}{\partial r}\right]B(r,r_n)\,\mathrm{d}r = \frac{2}{\pi\, r_n}\frac{\partial\overline{v}(r,q)}{\partial r}\bigg|_{r=R_1} - r_n^2\overline{v}_H(r_n,q), \tag{14}$$

we find that

$$\overline{v}_H(r_n,q) = \frac{2f\Gamma(a+1)}{\rho\pi r_n}\frac{1}{q^{a+1}(q+\lambda q^{\alpha+1}+\nu r_n^2)}. \tag{15}$$

Now, we rewrite Eq. (15) in the following equivalent form

$$\overline{v}_H(r_n,q) = \frac{2f\Gamma(a+1)}{\mu\pi r_n^3 q^{a+1}} - \frac{2f\Gamma(a+1)(1+\lambda q^{\alpha})}{\mu\pi r_n^3 q^{a}(q+\lambda q^{\alpha+1}+\nu r_n^2)}. \tag{16}$$

Applying the inverse Hankel transform to Eq. (16), and using the identity

$$\int_{R_1}^{R_2} r\ln\left(\frac{r}{R_2}\right)B(r,r_n)\,\mathrm{d}r = \frac{2}{\pi R_1 r_n^3}, \tag{17}$$

we obtain

$$\begin{aligned}\overline{v}(r,q) = {}& \frac{R_1 f\Gamma(a+1)}{\mu q^{a+1}}\ln\left(\frac{r}{R_2}\right) - \frac{\pi f\Gamma(a+1)}{\mu}\\ &\times\sum_{n=1}^{\infty}\frac{J_0^2(R_2r_n)B(r,r_n)}{r_n[J_1^2(R_1r_n) - J_0^2(R_2r_n)]}\frac{1+\lambda q^{\alpha}}{q^{a}[q+\lambda q^{\alpha+1}+\nu r_n^2]}.\end{aligned} \tag{18}$$

In order to obtain a suitable form for the velocity field $v(r,t)$, we rewrite the last factor from the second term of Eq. (18), into the equivalent form

$$\begin{aligned}\frac{1+\lambda q^{\alpha}}{q^{a}[q+\lambda q^{\alpha+1}+\nu r_n^2]} &= \frac{1+\lambda q^{\alpha}}{\lambda q^{a+1}[(q^{\alpha}+\frac{1}{\lambda})+(\frac{\nu r_n^2}{\lambda})q^{-1}]}\\ &= \frac{1}{\lambda}\sum_{k=0}^{\infty}\left(\frac{-\nu r_n^2}{\lambda}\right)^k\left[\frac{q^{-k-a-1}}{(q^{\alpha}+\lambda^{-1})^{k+1}}+\lambda\frac{q^{\alpha-k-a-1}}{(q^{\alpha}+\lambda^{-1})^{k+1}}\right].\end{aligned} \tag{19}$$

Introducing (19) into (18), and applying the discrete inverse Laplace transform, we find the velocity field under the form

$$v_a(r,t) = \frac{R_1}{\mu}\ln\left(\frac{r}{R_2}\right) f t^a - \frac{\pi f\Gamma(a+1)}{\mu\lambda}\sum_{n=1}^{\infty}\frac{J_0^2(R_2 r_n)B(r,r_n)}{r_n[J_1^2(R_1 r_n) - J_0^2(R_2 r_n)]}$$
$$\times \sum_{k=0}^{\infty}\left(\frac{-\nu r_n^2}{\lambda}\right)^k \left[G_{\alpha,-k-a-1,k+1}\left(\frac{-1}{\lambda},t\right) + \lambda G_{\alpha,\,\alpha-k-a-1,k+1}\left(\frac{-1}{\lambda},t\right)\right], \quad (20)$$

where the generalized $G_{a,b,c}(\cdot\,,\cdot)$ functions are defined by [25, Eqs. (101) and (99)]

$$G_{a,b,c}(d,t) = \mathcal{L}^{-1}\left\{\frac{q^b}{(q^a-d)^c}\right\} = \sum_{j=0}^{\infty}\frac{d^j\Gamma(c+j)}{\Gamma(c)\Gamma(j+1)}\frac{t^{(c+j)a-b-1}}{\Gamma[(c+j)a-b]}, \quad (21)$$
$$\operatorname{Re}(ac-b) > 0, \ \ \operatorname{Re}(q) > 0, \ \ \left|\frac{d}{q^a}\right| < 1.$$

3.2 Calculation of the shear stress

Applying the Laplace transform to Eq. (2b) we find that

$$\overline{\tau}(r,q) = \frac{\mu}{1+\lambda q^{\alpha}}\frac{\partial\overline{v}(r,q)}{\partial r}, \quad (22)$$

where

$$\frac{\partial\overline{v}(r,q)}{\partial r} = \frac{R_1 f\Gamma(a+1)}{\mu\, r\, q^{a+1}}$$
$$+ \frac{\pi f\Gamma(a+1)}{\mu}\sum_{n=1}^{\infty}\frac{J_0^2(R_2 r_n)\widetilde{B}(r,r_n)}{J_1^2(R_1 r_n) - J_0^2(R_2 r_n)}\frac{1+\lambda q^{\alpha}}{q^a[q+\lambda q^{\alpha+1}+\nu r_n^2]}, \quad (23)$$

is obtained from Eq. (18) and

$$\widetilde{B}(r,r_n) = J_1(r r_n)Y_1(R_1 r_n) - J_1(R_1 r_n)Y_1(r r_n). \quad (24)$$

Introducing (23) into (22), we get

$$\overline{\tau}(r,q) = \frac{R_1 f\Gamma(a+1)}{r(1+\lambda q^{\alpha})q^{a+1}}$$
$$+ \pi f\Gamma(a+1)\sum_{n=1}^{\infty}\frac{J_0^2(R_2 r_n)\widetilde{B}(r,r_n)}{J_1^2(R_1 r_n) - J_0^2(R_2 r_n)}\frac{1}{q^a[q+\lambda q^{\alpha+1}+\nu r_n^2]}. \quad (25)$$

By means of the identity

$$\frac{1}{q^a[q+\lambda q^{\alpha+1}+\nu r_n^2]} = \frac{1}{\lambda}\sum_{k=0}^{\infty}\left(\frac{-\nu r_n^2}{\lambda}\right)^k\left[\frac{q^{-k-a-1}}{(q^{\alpha}+\lambda^{-1})^{k+1}}\right], \quad (26)$$

Eq. (25) can be written in the form

$$\overline{\tau}(r,q) = \frac{R_1 f\Gamma(a+1)}{r(1+\lambda q^\alpha)q^{a+1}} + \frac{\pi f\Gamma(a+1)}{\lambda} \times \sum_{n=1}^{\infty} \frac{J_0^2(R_2 r_n)\widetilde{B}(r,r_n)}{J_1^2(R_1 r_n) - J_0^2(R_2 r_n)} \sum_{k=0}^{\infty} \left(\frac{-\nu r_n^2}{\lambda}\right)^k \left[\frac{q^{-k-a-1}}{(q^\alpha + \lambda^{-1})^{k+1}}\right]. \quad (27)$$

Now applying again the discrete inverse Laplace transform to Eq. (27) and using Eqs. (5) and (21), we find the shear stress $\tau(r,t)$ under the form

$$\tau_a(r,t) = \frac{R_1 f\Gamma(a+1)}{\lambda r} R_{\alpha,-a-1}\left(\frac{-1}{\lambda}, t\right) + \frac{\pi f\Gamma(a+1)}{\lambda} \times \sum_{n=1}^{\infty} \frac{J_0^2(R_2 r_n)\widetilde{B}(r,r_n)}{J_1^2(R_1 r_n) - J_0^2(R_2 r_n)} \sum_{k=0}^{\infty} \left(\frac{-\nu r_n^2}{\lambda}\right)^k G_{\alpha,-k-a-1,k+1}\left(\frac{-1}{\lambda}, t\right). \quad (28)$$

4 Limiting cases

4.1 Classical Maxwell fluid

Making $\alpha \to 1$ into Eqs. (20) and (28), we obtain the velocity field

$$v_{aM}(r,t) = \frac{R_1}{\mu} \ln\left(\frac{r}{R_2}\right) f t^a - \frac{\pi f\Gamma(a+1)}{\mu\lambda} \sum_{n=1}^{\infty} \frac{J_0^2(R_2 r_n)B(r,r_n)}{r_n[J_1^2(R_1 r_n) - J_0^2(R_2 r_n)]} \times \sum_{k=0}^{\infty} \left(\frac{-\nu r_n^2}{\lambda}\right)^k \left[G_{1,-k-a-1,k+1}\left(\frac{-1}{\lambda}, t\right) + \lambda G_{1,-k-a,k+1}\left(\frac{-1}{\lambda}, t\right)\right], \quad (29)$$

and the associated tangential stress

$$\tau_{aM}(r,t) = \frac{R_1 f\Gamma(a+1)}{\lambda r} R_{1,-a-1}\left(\frac{-1}{\lambda}, t\right) + \frac{\pi f\Gamma(a+1)}{\lambda} \times \sum_{n=1}^{\infty} \frac{J_0^2(R_2 r_n)\widetilde{B}(r,r_n)}{J_1^2(R_1 r_n) - J_0^2(R_2 r_n)} \sum_{k=0}^{\infty} \left(\frac{-\nu r_n^2}{\lambda}\right)^k G_{1,-k-a-1,k+1}\left(\frac{-1}{\lambda}, t\right), \quad (30)$$

corresponding to an ordinary Maxwell fluid performing the same motion.

Direct computations show that $v_{aM}(r,t)$ and $\tau_{aM}(r,t)$ satisfy the governing equations (2) with $\alpha = 1$ and all corresponding initial and boundary conditions.

More exactly, on the boundary we have

$$\tau_{aM}(R_1,t) = \frac{f\Gamma(a+1)}{\lambda} R_{1,-a-1}\left(\frac{-1}{\lambda}, t\right) \quad \text{and} \quad v_{aM}(R_2,t) = 0, \quad t \geq 0. \quad (31)$$

4.2 Newtonian fluid

By now letting $\lambda \to 0$ into Eqs. (29) and (30) and using the limit

$$\lim_{\lambda\to 0}\frac{1}{\lambda^k}G_{1,b,k}\left(\frac{-1}{\lambda},t\right)=\frac{t^{-b-1}}{\Gamma(-b)},\quad b<0,$$

we obtain the velocity field

$$v_{aN}(r,t)=\frac{R_1}{\mu}\ln\left(\frac{r}{R_2}\right)ft^a-\frac{\pi f\Gamma(a+1)}{\mu}\sum_{n=1}^{\infty}\frac{J_0^2(R_2r_n)B(r,r_n)}{r_n[J_1^2(R_1r_n)-J_0^2(R_2r_n)]}\times\sum_{k=0}^{\infty}(-\nu r_n^2)^k\frac{t^{k+a}}{\Gamma(k+a+1)}, \tag{32}$$

and the associated shear stress

$$\tau_{aN}(r,t)=\frac{R_1}{r}ft^a+\pi f\Gamma(a+1)\sum_{n=1}^{\infty}\frac{J_0^2(R_2r_n)\widetilde{B}(r,r_n)}{J_1^2(R_1r_n)-J_0^2(R_2r_n)}\times\sum_{k=0}^{\infty}(-\nu r_n^2)^k\frac{t^{k+a}}{\Gamma(k+a+1)}. \tag{33}$$

5 Special cases

5.1 Case $a=0$

By making $a=0$ in Eqs. (20), (28), (29), (30), (32) and (33), we recover the solutions (28), (33), (34), (35), (37) and (38) obtained in [27]. The corresponding velocities are

$$v_0(r,t)=\frac{R_1}{\mu}\ln\left(\frac{r}{R_2}\right)f-\frac{\pi f}{\mu\lambda}\sum_{n=1}^{\infty}\frac{J_0^2(R_2r_n)B(r,r_n)}{r_n[J_1^2(R_1r_n)-J_0^2(R_2r_n)]}\times\sum_{k=0}^{\infty}\left(\frac{-\nu r_n^2}{\lambda}\right)^k\left[G_{\alpha,-k-1,k+1}\left(\frac{-1}{\lambda},t\right)+\lambda G_{\alpha,\alpha-k-1,k+1}\left(\frac{-1}{\lambda},t\right)\right], \tag{34}$$

$$v_{0M}(r,t)=\frac{R_1}{\mu}\ln\left(\frac{r}{R_2}\right)f-\frac{\pi f}{\mu\lambda}\sum_{n=1}^{\infty}\frac{J_0^2(R_2r_n)B(r,r_n)}{r_n[J_1^2(R_1r_n)-J_0^2(R_2r_n)]}\times\sum_{k=0}^{\infty}\left(\frac{-\nu r_n^2}{\lambda}\right)^k\left[G_{1,-k-1,k+1}\left(\frac{-1}{\lambda},t\right)+\lambda G_{1,-k,k+1}\left(\frac{-1}{\lambda},t\right)\right], \tag{35}$$

$$v_{0N}(r,t)=\frac{R_1}{\mu}\ln\left(\frac{r}{R_2}\right)f-\frac{\pi f}{\mu}\sum_{n=1}^{\infty}\frac{J_0^2(R_2r_n)B(r,r_n)}{r_n[J_1^2(R_1r_n)-J_0^2(R_2r_n)]}e^{-\nu r_n^2t}. \tag{36}$$

From Fig. 1, it clearly results that $v_{0M}(r,t)$ given by Eq. (35) is equivalent with

$$v_{0M}(r,t) = \frac{R_1}{\mu}\ln\left(\frac{r}{R_2}\right)f - \frac{\pi f}{\mu}\sum_{n=1}^{\infty}\frac{J_0^2(R_2 r_n)B(r,r_n)}{r_n[J_1^2(R_1 r_n) - J_0^2(R_2 r_n)]}\frac{p_{2n}e^{p_{1n}t} - p_{1n}e^{p_{2n}t}}{p_{2n} - p_{1n}}, \tag{37}$$

obtained in [1] by a different technique. In Eq. (37)

$$p_{1n}, p_{2n} = \frac{-1 \pm \sqrt{1 - 4\nu\lambda r_n^2}}{2\lambda}.$$

The unsteady motion of Newtonian and Maxwell fluids as it results from Eqs. (36) and (37), ultimately becomes steady. Its starting solutions (36) and (37) (or equivalently (35)), describe the motion of the fluid some time after its initiation. After that time when the transient disappears, the motion of the fluid is described by the steady solution

$$v_{0MS}(r) = v_{0M}(r,\infty) = \frac{R_1}{\mu}\ln\left(\frac{r}{R_2}\right)f, \tag{38}$$

which is same for both kinds of fluids. The required time to reach the steady state for Maxwell fluids, as it results from Figs. 2 and 3, decreases for increasing λ. Consequently, the steady state is rather obtained for Newtonian fluids in comparison with Maxwell fluids.

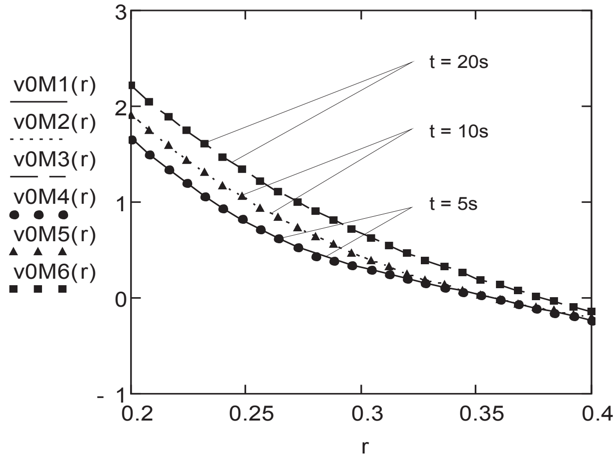

Fig. 1. Profiles of the velocities $v_{0M}(r,t)$ given by Eq. (35) – curves $v_{0M1}(r)$, $v_{0M2}(r)$, $v_{0M3}(r)$ and Eq. (37) – curves $v_{0M4}(r)$, $v_{0M5}(r)$, $v_{0M6}(r)$ for $R_1 = 0.2$, $R_2 = 0.4$, $f = -10$, $\mu = 0.466578$, $\nu = 0.000529$, $\lambda = 2$, and different values of t.

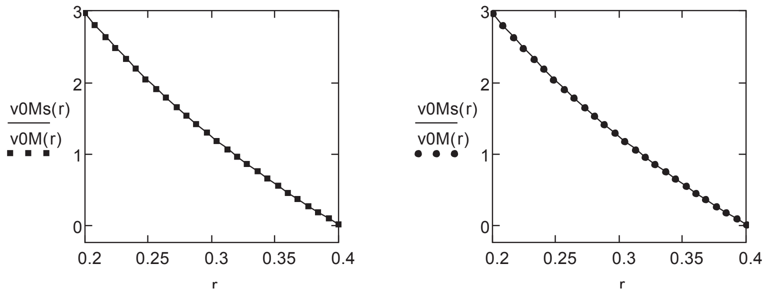

(a) $\lambda = 1, t = 160$ s (b) $\lambda = 4, t = 140$ s

Fig. 2. The required time to reach the steady-state for Maxwell fluids (case $a = 0$) for $R_1 = 0.2$, $R_2 = 0.4$, $f = -10$, $\mu = 0.466578$ and $\nu = 0.000529$.

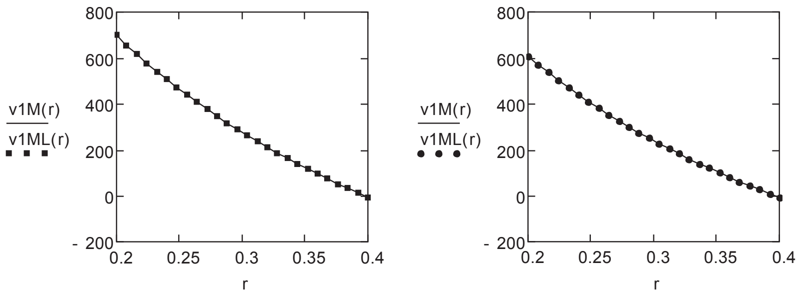

(a) $\lambda = 1, t = 250$ s (b) $\lambda = 4, t = 220$ s

Fig. 3. The required time to reach the steady-state for Maxwell fluids (case $a = 1$) for $R_1 = 0.2$, $R_2 = 0.4$, $f = -10$, $\mu = 0.466578$ and $\nu = 0.000529$.

5.2 Case $a = 1$

Taking $a = 1$ in Eqs. (20), (28), (29), (30), (32) and (33), we recover the solutions (23), (28), (29), (30), (32) and (33) obtained in [28]. The corresponding velocities are

$$v_1(r,t) = \frac{R_1}{\mu}\ln\left(\frac{r}{R_2}\right)ft - \frac{\pi f}{\mu\lambda}\sum_{n=1}^{\infty}\frac{J_0^2(R_2r_n)B(r,r_n)}{r_n[J_1^2(R_1r_n) - J_0^2(R_2r_n)]} \times \sum_{k=0}^{\infty}\left(\frac{-\nu r_n^2}{\lambda}\right)^k\left[G_{\alpha,-k-2,k+1}\left(\frac{-1}{\lambda},t\right) + \lambda G_{\alpha,\alpha-k-2,k+1}\left(\frac{-1}{\lambda},t\right)\right], \quad (39)$$

$$v_{1M}(r,t) = \frac{R_1}{\mu}\ln\left(\frac{r}{R_2}\right)ft - \frac{\pi f}{\mu\lambda}\sum_{n=1}^{\infty}\frac{J_0^2(R_2r_n)B(r,r_n)}{r_n[J_1^2(R_1r_n) - J_0^2(R_2r_n)]} \times \sum_{k=0}^{\infty}\left(\frac{-\nu r_n^2}{\lambda}\right)^k\left[G_{1,-k-2,k+1}\left(\frac{-1}{\lambda},t\right) + \lambda G_{1,-k-1,k+1}\left(\frac{-1}{\lambda},t\right)\right], \quad (40)$$

$$v_{1N}(r,t) = \frac{R_1}{\mu}\ln\left(\frac{r}{R_2}\right)ft - \frac{\pi f}{\mu\nu}\sum_{n=1}^{\infty}\frac{J_0^2(R_2r_n)B(r,r_n)}{r_n^3[J_1^2(R_1r_n) - J_0^2(R_2r_n)]}\left(1 - e^{-\nu r_n^2 t}\right). \quad (41)$$

From Fig. 4, it results that $v_{1M}(r,t)$ obtained in Eq. (40) is equivalent with

$$v_{1M}(r,t) = \frac{R_1}{\mu}\ln\left(\frac{r}{R_2}\right)ft - \frac{\pi f}{\mu\nu}\sum_{n=1}^{\infty}\frac{J_0^2(R_2r_n)B(r,r_n)}{r_n^3[J_1^2(R_1r_n) - J_0^2(R_2r_n)]}\left[1 + \lambda\frac{p_{2n}^2 e^{p_{1n}t} - p_{1n}^2 e^{p_{2n}t}}{p_{2n} - p_{1n}}\right], \quad (42)$$

obtained in [2] by a different technique. From Eqs. (36), (37) and (40), (41) it immediately results that

$$v_{1N}(r,t) = \int_0^t v_{0N}(r,s)\,\mathrm{d}s \quad \text{and} \quad v_{1M}(r,t) = \int_0^t v_{0M}(r,s)\,\mathrm{d}s. \quad (43)$$

Furthermore, $v_{1N}(r,t)$ and $v_{1M}(r,t)$ are presented as a sum between the transient solutions and the steady state solution

$$v_{1S}(r,t) = \frac{R_1}{\mu}\ln\left(\frac{r}{R_2}\right)ft - \frac{\pi f}{\mu\nu}\sum_{n=1}^{\infty}\frac{J_0^2(R_2r_n)B(r,r_n)}{r_n^3[J_1^2(R_1r_n) - J_0^2(R_2r_n)]}, \quad (44)$$

which is the same for both types of fluids.

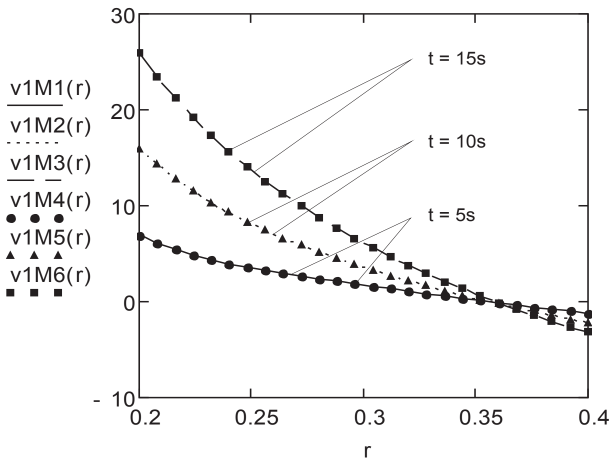

Fig. 4. Profiles of the velocities $v_{1M}(r,t)$ given by Eq. (40) – curves $v_{1M1}(r)$, $v_{1M2}(r)$, $v_{1M3}(r)$ and Eq. (42) – curves $v_{1M4}(r)$, $v_{1M5}(r)$, $v_{1M6}(r)$ for $R_1 = 0.2$, $R_2 = 0.4$, $f = -10$, $\mu = 0.466578$, $\nu = 0.000529$, $\lambda = 2$, and different values of t.

5.3 Case $a = 2$

By now letting $a = 2$ in Eqs. (20), (28), (29), (30), (32) and (33), we recover the corresponding solutions obtained in [29]. The corresponding velocities are

$$v_2(r,t) = \frac{R_1}{\mu}\ln\left(\frac{r}{R_2}\right)ft^2 - \frac{2\pi f}{\mu\lambda}\sum_{n=1}^{\infty}\frac{J_0^2(R_2r_n)B(r,r_n)}{r_n[J_1^2(R_1r_n) - J_0^2(R_2r_n)]} \times \sum_{k=0}^{\infty}\left(\frac{-\nu r_n^2}{\lambda}\right)^k\left[G_{\alpha,-k-3,k+1}\left(\frac{-1}{\lambda},t\right) + \lambda G_{\alpha,\alpha-k-3,k+1}\left(\frac{-1}{\lambda},t\right)\right], \quad (45)$$

$$v_{2M}(r,t) = \frac{R_1}{\mu}\ln\left(\frac{r}{R_2}\right)ft^2 - \frac{2\pi f}{\mu\lambda}\sum_{n=1}^{\infty}\frac{J_0^2(R_2r_n)B(r,r_n)}{r_n[J_1^2(R_1r_n) - J_0^2(R_2r_n)]} \times \sum_{k=0}^{\infty}\left(\frac{-\nu r_n^2}{\lambda}\right)^k\left[G_{1,-k-3,k+1}\left(\frac{-1}{\lambda},t\right) + \lambda G_{1,-k-2,k+1}\left(\frac{-1}{\lambda},t\right)\right], \quad (46)$$

$$v_{2N}(r,t) = \frac{R_1}{\mu}\ln\left(\frac{r}{R_2}\right)ft^2 - \frac{2\pi f}{\mu\nu}\sum_{n=1}^{\infty}\frac{J_0^2(R_2r_n)B(r,r_n)}{r_n^3[J_1^2(R_1r_n) - J_0^2(R_2r_n)]}\left[t - \frac{1}{\nu r_n^2}\left\{1 - e^{-\nu r_n^2 t}\right\}\right]. \quad (47)$$

By graphical illustrations it is shown in Fig. 5 the equivalence of $v_{2M}(r,t)$ given in Eq. (46) with

$$v_{2M}(r,t) = \frac{R_1}{\mu}\ln\left(\frac{r}{R_2}\right)ft^2 - \frac{2\pi f}{\mu\nu} \times \sum_{n=1}^{\infty}\frac{J_0^2(R_2r_n)B(r,r_n)}{r_n^3[J_1^2(R_1r_n) - J_0^2(R_2r_n)]}\left\{t + \lambda - \frac{1}{\nu r_n^2}\left[1 - \lambda^2\frac{p_{2n}^3e^{p_{1n}t} - p_{1n}^3e^{p_{2n}t}}{p_{2n} - p_{1n}}\right]\right\}, \quad (48)$$

obtained in [3]. From Eqs. (36), (37), (41), (42), (47) and (48), it is easy to see that

$$v_{2N}(r,t) = 2\int_0^t v_{1N}(r,s)\,\mathrm{d}s = 2\int_0^t\int_0^s v_{0N}(r,\tau)\,\mathrm{d}\tau\,\mathrm{d}s, \quad (49)$$

$$v_{2M}(r,t) = 2\int_0^t v_{1M}(r,s)\,\mathrm{d}s = 2\int_0^t\int_0^s v_{0M}(r,\tau)\,\mathrm{d}\tau\,\mathrm{d}s. \quad (50)$$

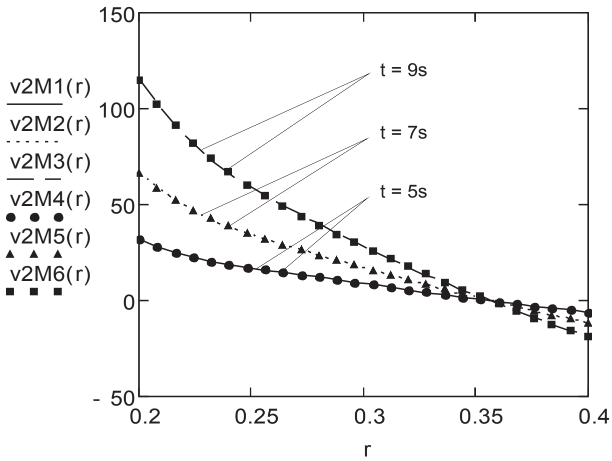

Fig. 5. Profiles of the velocities $v_{2M}(r,t)$ given by Eq. (46) – curves $v_{2M1}(r)$, $v_{2M2}(r)$, $v_{2M3}(r)$ and Eq. (48) – curves $v_{2M4}(r)$, $v_{2M5}(r)$, $v_{2M6}(r)$ for $R_1 = 0.2$, $R_2 = 0.4$, $f = -10$, $\mu = 0.466578$, $\nu = 0.000529$, $\lambda = 2$ and different values of t.

This property can be easily extended for any natural number a. Furthermore, a thorough analysis shows that the general solutions $v_n(r,t)$ as well as $\tau_n(r,t)$ satisfy the relations

$$v_n(r,t) = n! \int_0^t \int_0^{s_1} \int_0^{s_2} \dots \int_0^{s_{n-1}} v_0(r,s_n)\,\mathrm{d}s_n\,\mathrm{d}s_{n-1}\dots\mathrm{d}s_2\,\mathrm{d}s_1, \tag{51}$$

$$\tau_n(r,t) = n! \int_0^t \int_0^{s_1} \int_0^{s_2} \dots \int_0^{s_{n-1}} \tau_0(r,s_n)\,\mathrm{d}s_n\,\mathrm{d}s_{n-1}\dots\mathrm{d}s_2\,\mathrm{d}s_1. \tag{52}$$

Last relations (51) and (52) show the power of the solutions $v_0(r,t)$ and $\tau_0(r,t)$ corresponding to $a = 0$ in Eq. (7). All solutions corresponding to $a = 1,2,3,\dots$ can be presented as simple or multiple integrals of those corresponding to $a = 0$. We can extend the above relations for any positive real number a expressing in fractional integration

$$v_a(r,t) = \Gamma(a+1) D_t^{-a} v_0(r,t), \tag{53}$$

$$\tau_a(r,t) = \Gamma(a+1) D_t^{-a} \tau_0(r,t), \tag{54}$$

using

$$D_t^{-a} t^{\beta} = \frac{\Gamma(\beta+1)}{\Gamma(a+\beta+1)} t^{a+\beta}, \quad D_t^{-a} G_{a^*,b,c}(d,t) = G_{a^*,b-a,c}(d,t), \tag{55}$$

$$D_t^{-a} f(t) = \frac{1}{\Gamma(a)} \int_0^t (t-x)^{a-1} f(x)\,\mathrm{d}x, \quad a > 0, \tag{56}$$

so Eqs. (51) and (52) can be viewed as special cases of Eqs. (53) and (54), when a is a natural number.

6 Conclusions

In this paper, the unsteady motion of a fractional Maxwell fluid between two infinite coaxial circular cylinders is studied by means of the Laplace and finite Hankel transforms. The motion of the fluid is produced by the inner cylinder that, after the initial moment, is pulled with a time-dependent shear along its axis and the outer cylinder is held fixed. The velocity $v(r,t)$ and the adequate shear stress $\tau(r,t)$ are obtained under series form in terms of the generalized $G_{a,b,c}(.\,,t)$ and $R_{a,b}(.\,,t)$ functions. They satisfy all imposed initial and boundary conditions, and can immediately be particularized to give the similar solutions for ordinary Maxwell and Newtonian fluids. Furthermore, as it results from Eqs. (51) and (52), the solutions corresponding to $a = 1, 2, 3, \dots$ can be written as simple or multiple integrals of similar solutions for $a = 0$. As a check of obtained results, Figs. 1, 4 and 5 clearly show that the diagrams of our solutions (35), (40) and (46) for ordinary Maxwell fluids are almost identical to those obtained correspondingly in [1, 2] and [3] by a different technique. Other new and interesting results are:

1. The decay of the transient component in time, for velocity $v_{1M}(r,t)$ given in Eq. (42), is depicted in Fig. 6. It is clearly seen that the required time to reach the large-time state for velocity decreases if λ increases.
2. For $a = 0$, profiles of the velocities for fractional Maxwell and ordinary Maxwell fluids are depicted together for three different values of time in Fig 7. From this it is clearly indicated that for all values of time t, ordinary Maxwell fluid is the slowest and fractional Maxwell fluid is the fastest. The units of the material constants in Figs. 1–7 are SI units and, the roots r_n have been approximated by $(2n-1)\pi/[2(R_2 - R_1)]$.

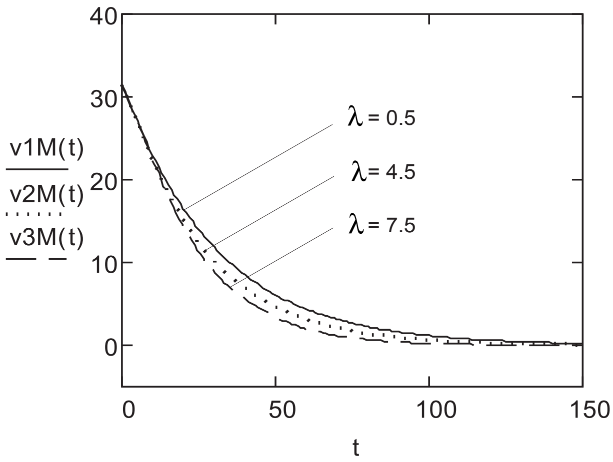

Fig. 6. Decay of the transient component of the velocity $v_{1M}(r,t)$ given by Eq. (42) for $R_1 = 0.2$, $R_2 = 0.4$, $f = -10$, $\mu = 0.466578$, $\nu = 0.000529$ and different values of λ.

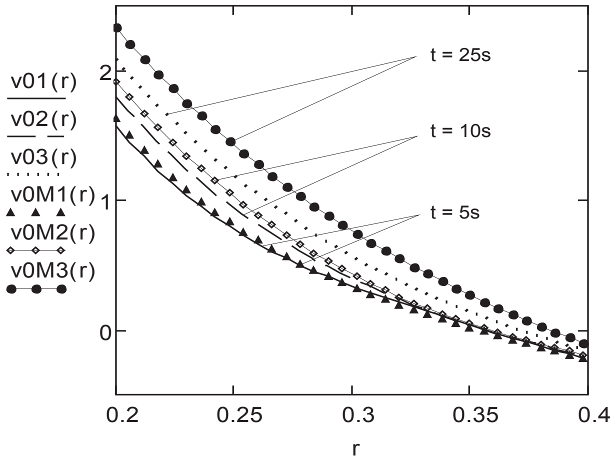

Fig. 7. Profiles of the velocities $v_0(r,t)$ given by Eq. (34) – curves $v_{01}(r,t)$, $v_{02}(r,t)$, $v_{03}(r,t)$ and $v_{0M}(r,t)$ given by Eq. (35) – curves $v_{0M1}(r,t)$, $v_{0M2}(r,t)$, $v_{0M3}(r,t)$ for $R_1 = 0.2$, $R_2 = 0.4$, $f = -10$, $\mu = 0.466578$, $\nu = 0.000529$, $\lambda = 2$, $\alpha = 0.4$ and different values of t.

Acknowledgement

The authors would like to express their gratitude to the referees for their careful assessment, constructive comments and criticism for the improvement of the initial form of the manuscript.

The authors are also thankful to Abdus Salam School of Mathematical Sciences, GC University, Lahore, Pakistan; COMSATS Institute of Information Technology, Wah Cantt, Pakistan; and Higher Education Commission of Pakistan for supporting and facilitating this research work.

References

1. Corina Fetecau, A.U. Awan, Mehwish Rana, Axial-Couette flow of an Oldroyd-B fluid in an annulus due to a time-dependent shear stress, *Meccanica*, Article ID MECC673 (submitted).

2. M. Jamil, C. Fetecau, Heical flows of Maxwell fluid between coaxial cylinders with given shear stresses on the boundary, *Nonlinear Anal. Real World Appl.*, **11**, pp. 4302–4311, 2010.

3. M. Jamil, C. Fetecau, N.A. Khan, A. Mahmood, Some exact solutions for helical flows of Maxwell fluid in an annular pipe due to accelerated shear stresses, *International Journal of Chemical Reactor Engineering*, **9**, A20, 2011.

4. Z.S. Yu, J.Z. Lin, Numerical research on the coherent structure in the viscoelastic second-order mixing layers, *Appl. Math. Mech.*, **8**, pp. 717–723, 1998.

5. T.W. Ting, Certain non-steady flows of second-order fluids, *Arch. Ration. Mech. An.*, **14**, pp. 1–23, 1963.
6. P.H. Srivastava, Non-steady helical flow of a visco-elastic liquid, *Arch. Mech. Stos.*, **18**, pp. 145–150, 1966.
7. N.D. Waters, M.J. King, Unsteady flow of an elastico-viscous liquid in a straight pipe of circular cross-section, *J. Phys. D Appl. Phys.*, **4**, pp. 207–211, 1971.
8. R. Bandelli, K.R. Rajagopal, Start-up flows of second grade fluids in domains with one finite dimension, *Int. J. Non-Linear Mech.*, **30**, pp. 817–839, 1995.
9. R. Bandelli, K.R. Rajagopal, G.P. Galdi, On some unsteady motions of fluids of second grade, *Arch. Mech.*, **47**, pp. 661–676, 1995.
10. N.D. Waters, M.J. King, Unsteady flow of an elastico-viscous liquid, *Rheol. Acta*, **9**, pp. 345–355, 1970.
11. Corina Fetecau, C. Fetecau, M. Imran, Axial Couette flow of an Oldroyd-B fluid due to a time-dependent shear stress, *Math. Reports*, **11**(61), 145–154, 2009.
12. Corina Fetecau, M. Imran, C. Fetecau, I. Burdujan, Helical flow of an Oldroyd-B fluid due to a circular cylinder subject to time-dependent shear stresses, *Z. Angew. Math. Phys.*, **61**, pp. 959–969, 2010.
13. P.E. Rouse, The theory of the linear viscoelastic properties of dilute solutions of coiling polymers, *J. Chem. Phys.*, **21**, pp. 1272–1280, 1953.
14. J.D. Ferry, R.F. Landel, M.L. Williams, Extensions of the Rouse theory of viscoelastic properties to undiluted linear polymers, *J. Appl. Phys.*, **26**, pp. 395–362, 1995.
15. D. Tong, R. Wang, H. Yang, Exact solutions for the flow of non-Newtonian fluid with fractional derivative in an annular pipe, *Sci. China Ser. G*, **48**, pp. 485–495, 2005.
16. D. Tong, Y. Liu, Exact solutions for the unsteady rotational flow of non-Newtonian fluid in an annular pipe, *Int. J. Eng. Sci.*, **43**, pp. 281–289, 2005.
17. C. Fetecau, A. Mahmood, Corina Fetecau, D. Vieru, Some exact solutions for the helical flow of a generalized Oldroyd-B fluid in a circular cylinder, *Comput. Math. Appl.*, **56**, pp. 3096–3108, 2008.
18. S. Wang, M. Xu, Axial Coutte flow of two kinds of fractional viscoelastic fluids in an annulus, *Nonlinear Anal. Real World Appl.*, **10**(2), pp. 1087–1096, 2009.
19. A. Heibig, L.I. Palade, On the rest state stability of an objective fractional derivative viscoelastic fluid model, *J. Math. Phys.*, **49**, pp. 04310-1–22, 2008.
20. L.I. Palade, R.R. Attané, P. Huilgol, B. Mena, Anomalous stability behavior of a properly invariant constitutive equation which generalise fractional derivative models, *Int. J. Eng. Sci.*, **37**, pp. 315–329, 1999.
21. J. Sabatier, O.P. Agrawal, J.A.T. Machado, *Advances in Fractional Calculus: Theoretical Developments and Applications in Physics and Engineering*, Springer, Netherland 2007.

22. A. Carpinteri, F. Mainardi, *Fractals and Fractional Calculus in Continum Mechanics*, Springer, New York 1997.

23. S.G. Samko, A.A. Kilbas, O.I. Marichev, *Fractional Integrals and Derivatives: Theory and Applications*, Gordon and Breach, Amsterdom, 1993.

24. I. Podlubny, *Fractional Differential Equations*, Academic Press, San Diego, 1999.

25. C.F. Lorenzo, T.T. Hartley, Generalized Functions for Fractional Calculus, NASA/TP-1999-209424, 1999.

26. L. Debnath, D. Bhatta, *Integral Transforms and Their Applications*, 2nd edition, Chapman & Hall/CRC, 2007.

27. C. Fetecau, A. Mahmood, M. Jamil, Exact solutions for the flow of a viscoelastic fluid induced by a circular cylinder subject to a time-dependent shear stress, *Commun. Nonlinear Sci. Numer. Simul.*, **15**, pp. 3931–3938, 2010.

28. M. Jamil, A. Mahmood, C. Fetecau, Corina Fetecau, Exact solutions for the unsteady flow of a generalized Maxwell fluid in an annulus due to a longitudinal time-dependent shear stress, *Arch. Mech.* (submitted 81/2010/f).

29. M. Jamil, C. Fetecau, Corina Fetecau, A. Mahmood, Flow of fractional Maxwell fluid between coaxial cylinders, *Arch. Appl. Mech.*, DOI 10.1007/s00419-011-0536-x, 2011.